AD-A182 436 EPR (ELECTRON PARAMAGNETIC RESONANCE) STUDIES OF DEFECTS AND IMPURITIES I (U) AEROSPACE CORP EL SEGUNDO CA CHEMISTRY AND PHYSICS LAB R C BOWMAN ET AL 1/1

UNCLASSIFIED 22 MAY 87 TR-0086(6945-07)-2 SD-TR-87-23 F/G 7/2 NL

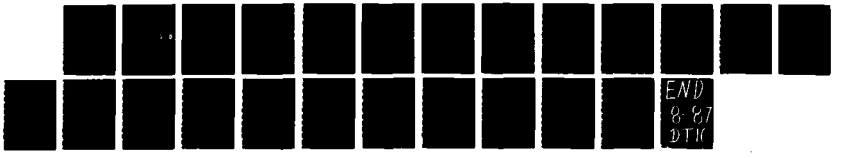

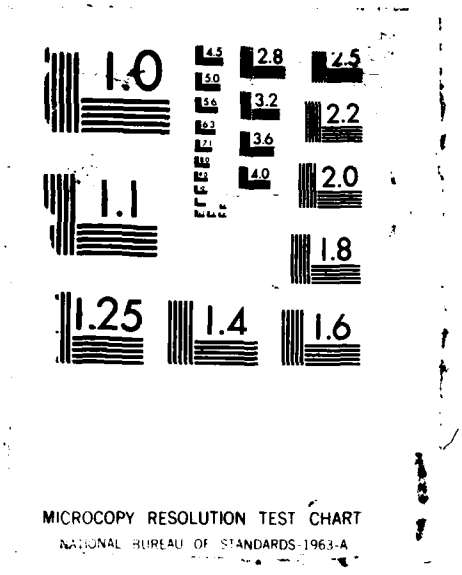
1.0
1.1
1.25
1.4
1.6
1.8
2.0
2.2
2.5
2.8
3.2
3.6
4.0
4.5
5.0
5.6
6.3
7.1
8.0
MICROCOPY RESOLUTION TEST CHART
NATIONAL BUREAU OF STANDARDS-1963-A

REPORT SD-TR-87-23

EPR Studies of Defects and Impurities in Boron-Implanted $Hg_{1-x}Cd_xTe$

Prepared by

ROBERT C. BOWMAN, JR.
Chemistry and Physics Laboratory
Laboratory Operations
The Aerospace Corporation
El Segundo, CA 90245

and

E. L. VENTURINI
Sandia National Laboratories
Albuquerque, NM 87185

22 May 1987

Prepared for

SPACE DIVISION
AIR FORCE SYSTEMS COMMAND
Los Angeles Air Force Station
P.O. Box 92960, Worldway Postal Center
Los Angeles, CA 90009-2960

This report was submitted by The Aerospace Corporation, El Segundo, CA 90245, under Contract No. F04701-85-C-0086 with the Space Division, P.O. Box 92960, Worldway Postal Center, Los Angeles, CA 90009-2960. It was reviewed and approved for The Aerospace Corporation by S. Feuerstein, Director, Chemistry and Physics Laboratory. Lt Walter E. Leyland, CNDA, was the project officer for the Mission-Oriented Investigation and Experimentation (MOIE) program.

This report has been reviewed by the Public Affairs Office (PAS) and is releasable to the National Technical Information Service (NTIS). At NTIS, it will be available to the general public, including foreign nationals.

This technical report has been reviewed and is approved for publication. Publication of this report does not constitute Air Force approval of the report's findings or conclusions. It is published only for the exchange and stimulation of ideas.

Walter E Leyland

WALTER E. LEYLAND, Lt, USAF
MOIE Project Officer
SD/CNDA

JOSEPH HESS, GM-15
Director, AFSTC West Coast Office
AFSTC/WCO OL-AB

UNCLASSIFIED

SECURITY CLASSIFICATION OF THIS PAGE

REPORT DOCUMENTATION PAGE

A182436

1a. REPORT SECURITY CLASSIFICATION Unclassified	1b. RESTRICTIVE MARKINGS
2a. SECURITY CLASSIFICATION AUTHORITY	3. DISTRIBUTION/AVAILABILITY OF REPORT Approved for public release; distribution unlimited.
2b. DECLASSIFICATION/DOWNGRADING SCHEDULE	
4. PERFORMING ORGANIZATION REPORT NUMBER(S) TR-0086(6945-07)-2	5. MONITORING ORGANIZATION REPORT NUMBER(S) SD-TR-87-23
6a. NAME OF PERFORMING ORGANIZATION The Aerospace Corporation Laboratory Operations 6b. OFFICE SYMBOL (If applicable)	7a. NAME OF MONITORING ORGANIZATION Space Division
6c. ADDRESS (City, State and ZIP Code) El Segundo, CA 90245	7b. ADDRESS (City, State and ZIP Code) Los Angeles Air Force Station Los Angeles, CA 90009-2960
8a. NAME OF FUNDING/SPONSORING ORGANIZATION 8b. OFFICE SYMBOL (If applicable)	9. PROCUREMENT INSTRUMENT IDENTIFICATION NUMBER F04701-85-C-0086
8c. ADDRESS (City, State and ZIP Code)	10. SOURCE OF FUNDING NOS. PROGRAM ELEMENT NO. / PROJECT NO. / TASK NO. / WORK UNIT NO.
11. TITLE (Include Security Classification) EPR Studies of Defects and Impurities in	
12. PERSONAL AUTHOR(S) Bowman, Robert C., Jr., and Venturini, E. L.(Sandia National Laboratories)	
13a. TYPE OF REPORT 13b. TIME COVERED FROM _____ TO _____	14. DATE OF REPORT (Yr., Mo., Day) 1987 May 22 15. PAGE COUNT 18
16. SUPPLEMENTARY NOTATION Sandia National Laboratories are operated for the U.S. Department of Energy under Contract No. DE-AC04-76P00789.	
17. COSATI CODES FIELD / GROUP / SUB. GR.	18. SUBJECT TERMS (Continue on reverse if necessary and identify by block number) Mercury cadmium telluride, Electron paramagnetic resonance, Ion implantation damage, Defects in semiconductors

19. ABSTRACT (Continue on reverse if necessary and identify by block number)

Representative high-purity single crystals of $Hg_{1-x}Cd_xTe$ have been examined by electron paramagnetic resonance (EPR) to determine whether they contain Fe^{+3} impurities or defects. EPR spectra consistent with substitutional Fe^{+3} impurities were obtained from some CdTe samples, but no paramagnetic centers have been observed in p-type $Hg_{0.7}Cd_{0.3}Te$. Since boron ion-implantation is commonly used to produce n-p junctions in HgCdTe during the fabrication of infrared sensor devices, paramagnetic damage centers are likely to form but have not been previously demonstrated. We report the observation of "free-electron"-like EPR signals in heavily $^{11}B^+$ implanted CdTe and $Hg_{0.7}Cd_{0.3}Te$. These spectra have similar EPR characteristics to the so-called dangling-bond defects generated in ion-implanted Si and GaP. Although the identities of these defects in HgCdTe remain to be established, the effects of implant conditions and thermal treatments are briefly described.

20. DISTRIBUTION/AVAILABILITY OF ABSTRACT UNCLASSIFIED/UNLIMITED ☒ SAME AS RPT ☐ DTIC USERS ☐	21. ABSTRACT SECURITY CLASSIFICATION Unclassified
22a. NAME OF RESPONSIBLE INDIVIDUAL	22b. TELEPHONE NUMBER (Include Area Code) 22c. OFFICE SYMBOL

DD FORM 1473, 83 APR EDITION OF 1 JAN 73 IS OBSOLETE.

UNCLASSIFIED

SECURITY CLASSIFICATION OF THIS PAGE

Block 11 (Continued)

Boron-Implanted $Hg_{1-x}Cd_xTe$

PREFACE

We wish to thank Prof. S. I. Chan and S. N. Witt for making available the EPR spectrometer at Caltech, R. E. Robertson for assistance with the sample handling, and Dr. J. F. Knudsen for the ion implantation.

CONTENTS

FIGURES

TABLES

I. INTRODUCTION

Electron paramagnetic resonance (EPR) spectroscopy, which is also known as electron spin resonance (ESR), has been widely used to characterize defects and impurities in semiconductors. The basic theoretical foundations and experimental methods of EPR are very well documented in standard texts.[1,2] The unpaired electron spins that are detected in the EPR experiments experience numerous interactions which are represented by a spin Hamiltonian ($\mathcal{H}_s$) as

$$\mathcal{H}_s = \beta \underset{\sim}{H}\cdot\underset{\sim}{g}\cdot\underset{\sim}{S} + \underset{\sim}{S}\cdot\underset{\sim}{D}\cdot\underset{\sim}{S} + \underset{\sim}{I}\cdot\underset{\sim}{A}\cdot\underset{\sim}{S} + \sum_n \underset{\sim}{I}_n\cdot\underset{\sim}{A}_n\cdot\underset{\sim}{S}. \qquad (1)$$

The first term represents the Zeeman interaction between unpaired electrons (spin quantum number $\underset{\sim}{S}$) and an applied magnetic field $\underset{\sim}{H}$, where β is the Bohr magnetron and $\underset{\sim}{g}$ is the g-factor tensor. The second term provides a general representation[1] of interactions with orbital angular momentum of the excited electronic states. The third term is the magnetic interaction between unpaired electrons and their own nucleus of spin $\underset{\sim}{I}$, where $\underset{\sim}{A}$ is the hyperfine tensor. The last term corresponds to magnetic interactions between the electrons and nuclear moments located at n different lattice sites (usually nearest neighbors), which give rise to the superhyperfine tensors $\underset{\sim}{A}_n$. There can be some additional terms to Eq. (1), but they are not usually relevant to the present situation. The explicit form of the spin Hamiltonian in any particular case is dependent upon the symmetry of the paramagnetic center. Consequently, magnitudes and crystallographic orientation dependences of the experimental g-factor, fine structure, and hyperfine tensors can unequivocally identify the paramagnetic center in favorable cases. Some typical paramagnetic defects found in semiconductors are listed in Table I. Numerous factors influence the extent to which EPR spectra can be analyzed, and resolved hyperfine splittings are usually required for detailed interpretations. However, EPR is of limited value for diamagnetic species unless that defect or impurity can be made paramagnetic by light illumination or other type of

TABLE I. COMMONLY OBSERVED PARAMAGNETIC SPECIES IN SEMICONDUCTORS

1. Conduction Electrons
2. Shallow Donor States
3. Shallow Acceptor States (Difficult to Observe)
4. Intrinsic Defects
   - A. Vacancies
   - B. Interstitials
   - C. Antisites (Common for III-V, possible in II-VI)
5. Transition-Metal Impurities
6. "Dangling-Bond" Defects--Amorphous, surface, and radiation damaged regions
7. Impurity-Defect Complexes

excitation-ionization process. The radiation damage from high-energy photons, neutrons, or ion implantation treatments will often generate various paramagnetic defects that include the so-called dangling bonds created by the rupture of covalent chemical bonds within the solid.

Although EPR studies have been conducted on numerous II-VI compound semiconductors,[3-5] rather limited EPR data appears to be currently available for the $Hg_{1-x}Cd_xTe$ system. Table II provides summaries of the absolute g-values, isotopic hyperfine coefficients (A_{iso}), and peak-to-peak linewidths (ΔH_{pp}) for most of the simple defects in CdTe where the EPR data are taken from the literature. The original references are footnoted in Table II. To the best of our knowledge, only two papers[6,7] have presented any EPR data for the $Hg_{1-x}Cd_xTe$ alloys. It was rather surprising to find such limited published EPR results on these technologically important materials, for which defects and impurities are widely held[7] to dominate many of the electronic properties and device performance parameters. Consequently, we decided to examine representative "high-purity" single crystal $Hg_{1-x}Cd_xTe$ samples from different sources. The intent was to determine whether these materials contain any paramagnetic residual impurities or intrinsic defects (i.e.,

TABLE II. CHARACTERISTICS OF EPR SPECTRA FOR IMPURITIES AND SIMPLE DEFECTS IN CdTe AS COMPILED FROM THE OPEN LITERATURE

SPECIES	T (K)	|g|	A_{iso} ($10^{-4}cm^{-1}$)	ΔH_{pp} (gauss)	LIGHT ACTIVE	REFERENCE
Mn^{+2}	4.2	2.010	55		?	a
Cr^{+}	1.4	1.997(3)	12.78(5)		?	b
Cr^{+2}	4.2	1.980(15)			?	c
Co^{+2}	10	2.3093	23.4		?	d
$^{205}Tl^{+2}$	77	2.035	17,900(100)		NO	e
V_{Cd}(?)	4	1.830(2)		~17	YES	f
V_{Te}(?)	4	2.003		~16	NO	f
Donor(Cl)	12	1.668(1)		25	YES	g
Donor(In)	12	1.704(1)		80	YES	g
Fe^{+3}	4.2	2.084(1)		$\geq$5	YES	h
Ni^{+}	4.1	1.425	81.7	$\overline{2}$3	NO	i
Pb^{+3}	20	2.1451(7)	205(10)		YES	j
Sn^{+3}	20	2.1012(7)	3934(10)		YES	j
Ge^{+3}	20	2.2054(7)	4884(10)		YES	j

[a] J. Lambe and C. Kikuchi, Phys. Rev. 119, 1256 (1960).
[b] C. W. Ludwig and M. R. Lorenz, Phys. Rev. 131, 601 (1963).
[c] J. T. Vallin and G. D. Watkins, Solid State Commun. 9, 953 (1971).
[d] F. S. Ham, et al., Phys. Rev. Lett. 5, 468 (1960).
[e] R. C. DuVarney and A. K. Garrison, Phys. Rev. B 12, 10 (1975).
[f] A. Goltzene and C. Schwab, Rev. Phys. Appl. (Paris) 12, 199 (1977).
[g] K. Saminadayar, D. Galland, and E. Molva, Solid State Commun. 49, 627 (1984).
[h] G. Brunthaler, U. Kaufmann, and J. Schneider, J. Appl. Phys. 56, 2974 (1984).
[i] U. Kaufmann, J. Windscheif, and G. Brunthaler, J. Phys. C: Solid State Phys. 17, 6169 (1984).
[j] G. Brunthaler, et al., Phys. Rev. B 31, 1239 (1985).

vacancies, interstitials, or antisite atoms). In fact, transition metals were found in some CdTe crystals, but no paramagnetic species have yet been observed in as-prepared n- or p-type $Hg_{0.7}Cd_{0.3}Te$.

Ion implantation has extensive applications in the fabrication of IR sensor devices. Implantations always appear to generate an n-type layer in $Hg_{1-x}Cd_xTe$. However, the nature of these donor species has not been concretely established, although they are widely believed[8,9] to be "defects" and not the implanted ions themselves. Thermal anneals apparently can activate some implanted ions to show[9] either donor (e.g., In) or acceptor (e.g., P) behavior; yet, many issues remain unresolved. In particular, the behavior of implanted boron (B) atoms, which are expected to be donors when substituted on the metal sites in $Hg_{1-x}Cd_xTe$, remains very controversial. Several authors[8,9] have questioned whether the boron ions play any direct role in the formation of the n-p junction. As shown in Table II, characteristic EPR spectra have been observed in CdTe for both shallow donors (i.e., Cl, In, and Al) and deep donors (i.e., Tl, Pb, Sn, Ge, and Fe). Consequently, EPR experiments have been performed on boron-implanted CdTe and $Hg_{0.7}Cd_{0.3}Te$ to determine the possible presence of donor states or other paramagnetic radiation damage centers created during implantation. In fact, a rather intense EPR signal with "free-electron"-like characteristics has been observed. Although the specific defect (or, possibly, defects) responsible for this new signal has not been identified, it appears to be very similar to the "dangling-bond" centers reported for ion implanted Si[10] and GaP.[11] Studies on the annealing behavior have been initiated, and the progress will be briefly described.

II. EXPERIMENTAL DETAILS

The $Hg_{1-x}Cd_xTe$ single crystals used in the EPR experiments were nominally undoped bulk pieces with approximate dimensions 3 mm × 10-20 mm × 0.5-1.0 mm. The CdTe crystals were obtained from II-VI Inc., and Cominco and New England Research Corporation were the sources of the $Hg_{1-x}Cd_xTe$ wafers. While the semi-insulating (SI) CdTe and two of the $Hg_{0.7}Cd_{0.3}Te$ samples had known orientations for the major face, most of the $Hg_{1-x}Cd_xTe$ crystals had been sliced at random orientations. Some properties of these samples are summarized in Table III. It should be noted that the hole carrier contents vary by about an order of magnitude for the p-$Hg_{0.7}Cd_{0.3}Te$ samples.

Two X-band (i.e., about 9 GHz) spectrometers were used for the EPR measurements. A Varian E-line spectrometer with a window in the microwave cavity to permit in situ illumination of the samples at temperatures down to about 5 K was used in the Noyes Laboratory of the California Institute of Technology. A home-built homodyne spectrometer at Sandia National Laboratories (SNLA) permitted in-dark EPR measurements to about 2 K. The prior calibrations of the SNLA spectrometer readily gave accurate g-values and lineshape parameters as well as spin concentrations.

The boron ($^{11}B^+$) ion implantations were done at The Aerospace Corporation with a 400 MPR-Veeco/AI system. In order to facilitate comparisons of boron implant effects, several samples (i.e., C1, C3, H5, H6, and H7) were simultaneously implanted in a single run with the samples at room temperature and a low dose rate to minimize heating. Since the implant range is dependent upon the ion's kinetic energy, this implant consisted of four stages where 2.5×10^{15} B^+ ions/cm^2 were implanted with 100 keV, 200 keV, 300 keV, and 400 keV to give a final cumulative dose of 1×10^{16} B^+ ions/cm^2. These conditions are expected[12] to produce a fairly uniform (although the boron concentrations will decrease with distance from implant surface) ^{11}B distribution for more than a 1.0 μm thick layer into the $Hg_{1-x}Cd_xTe$ crystals. The n-p junction will probably be somewhat deeper,[13] but its position has not yet been determined for any of these samples. The primary intent was to create reasonably large

volumes of implant and damage regions so that any paramagnetic centers could be detected by the available EPR equipment.

TABLE III. SUMMARY OF $Hg_{1-x}Cd_xTe$ SAMPLES USED IN EPR STUDIES AND OVERVIEW OF OBSERVATIONS ON AS-PREPARED CRYSTALS

SAMPLE I.D.	NOMINAL COMPOSITION	TYPE	x	CARRIERS[a] ($10^{15}cm^{-3}$)	MOBILITY[a] ($cm^2/V \cdot s$)	INITIAL EPR RESULTS
C1	<111>-CdTe	SI	1.00			Fe^{+3}, Co^{+2}
C2	<111>-CdTe	SI	1.00			Fe^{+3}
C3	<100>-CdTe	SI	1.00			Nothing found (w/wo light)
H1	$Hg_{0.7}Cd_{0.3}Te$	p	0.34	82	120	Nothing found (w/wo light)
H2	$Hg_{0.7}Cd_{0.3}Te$	p	0.282	16	260	Nothing found (w/wo light)
H3	$Hg_{0.6}Cd_{0.4}Te$	n	0.405	0.18	15,000	Nothing found (w/wo light)
H4	$Hg_{0.7}Cd_{0.3}Te$	n	0.292	0.14	67,000	Could not tune
H5	<110>$Hg_{0.7}Cd_{0.3}Te$	p	0.318	0.9	400	Nothing
H6	<110>-$Hg_{0.7}Cd_{0.3}Te$	p	0.318	60		Nothing (tuning difficult)
H7	$Hg_{0.7}Cd_{0.3}Te$	p	0.31	1.3	290	Nothing

[a]From 77 K Hall data supplied by the vendors.

III. RESULTS AND DISCUSSIONS

The results of the present X-band EPR measurements at low temperature (i.e., $T \leq 77$ K) for as-received $Hg_{1-x}Cd_xTe$ crystals are summarized in Table III. The possible presence of the previously observed paramagnetic centers listed in Table II, as well as any unidentified species, was considered. Two of the CdTe samples exhibited rather sharp and highly anisotropic EPR peaks that are characteristic of Fe^{+3} ions on the metal sites. One sample (i.e., C1) also gave a very weak isotropic spectrum with eight hyperfine components that approximately match the Co^{+2} parameters in Table II. No EPR signals were observed for the CdTe sample C3 nor any of the p-type $Hg_{0.7}Cd_{0.3}Te$ and n-type $Hg_{0.6}Cd_{0.4}Te$ samples. Even when crystals were cooled to temperatures below 15 K, in situ illumination with UV-filtered and IR-filtered lamps and an unfiltered xenon lamp had no noticeable effect upon the EPR signals for any of these samples. In particular, we saw no evidence for the $g = 2.35 - 2.5$ or $g = 3.0$ centers reported by Jones, et al.[7] for undoped p-$Hg_{0.7}Cd_{0.3}Te$, although the acceptor contents in our samples varied by a factor of 10. Of course, many factors can preclude[1,2] the observation of the EPR spectra, although considerable effort was made to vary the operating conditions so that paramagnetic species could be detected. The high electrical conductivity of the n-type H4 sample made it impossible to tune the microwave cavity, which prevented any EPR measurements. Similar, though less severe, tuning problems were encountered with some of the narrow-gap $Hg_{1-x}Cd_xTe$ samples both before and after ion implantation. While the present results indicate the absence of paramagnetic impurities and defects in these particular samples (except for the CdTe samples C1 and C2), they cannot provide information on diamagnetic centers that were not activated during the rather simple conditions employed. Furthermore, samples from other HgCdTe sources that include epitaxially grown films need to be examined before more general conclusions are reached on the possible existence of intrinsic paramagnetic defects (e.g., vacancies or antisites).

No new EPR signals were observed when CdTe or $Hg_{0.7}Cd_{0.3}Te$ crystals were implanted with 40 keV and/or 100 keV boron ions with total doses up to 2×10^{15} ions/cm^2. However, sharp, nearly isotropic signals at magnetic fields corresponding to g = 2.00 were obtained after the four energy implants described above, to give a total dose of 1×10^{16} ions/cm^2. Representative examples of the implantation-induced EPR spectra for CdTe and $Hg_{0.7}Cd_{0.3}Te$ are presented in Figs. 1 and 2, respectively. These B-implanted samples gave similar EPR traces at 77 K, whereas no signals were apparent from unimplanted crystals. The spectra for implanted $Hg_{0.7}Cd_{0.3}Te$ samples are seen to have narrower peak widths (ΔH_{pp}) as well as somewhat greater intensities. That the intensity of the EPR signals from the $Hg_{0.7}Cd_{0.3}Te$ samples is usually larger than EPR spectra observed from CdTe crystals which were identically implanted implies a tendency of $Hg_{0.7}Cd_{0.3}Te$ to form more defects during implantation. The EPR parameters for the implant-induced centers in the CdTe and $Hg_{0.7}Cd_{0.3}Te$ samples are summarized in Table IV along with the similar characteristics reported[10,11] for the dangling-bond defects in ion-implanted Si and GaP. The g-factors for all the implanted $Hg_{1-x}Cd_xTe$ samples are equivalent within experimental accuracy and are nearly identical to the free-electron value $g_e = 2.0023$. While these g-factors may be slightly anisotropic, Δg appears to be less than 4×10^{-4}. As shown in Figs. 1 and 2, the lineshapes in $Hg_{1-x}Cd_xTe$ are nearly Lorentzian for temperatures above 4 K. The ΔH_{pp} values are smaller for the $Hg_{0.7}Cd_{0.3}Te$ samples than for the implanted CdTe crystals. If the lineshapes are primarily determined by the electron spin exchange mechanism,[1] the narrower ΔH_{pp} values for $Hg_{0.7}Cd_{0.3}Te$ imply a stronger exchange coupling due to either a higher density of paramagnetic centers or a larger delocalization of the spin wavefunctions than for CdTe. Although a firm conclusion cannot be currently reached, the more intense EPR signals in the $Hg_{0.7}Cd_{0.3}Te$ samples favor the first alternative. The measured temperature-dependences of the EPR signals for the implanted $Hg_{1-x}Cd_xTe$ follow the inversed Curie behavior expected for isolated spins rather than the temperature-independent Pauli intensities predicted for conduction electrons. Hence, the observed EPR spectra caused by the boron implants do not directly correspond to the degenerate conduction bands

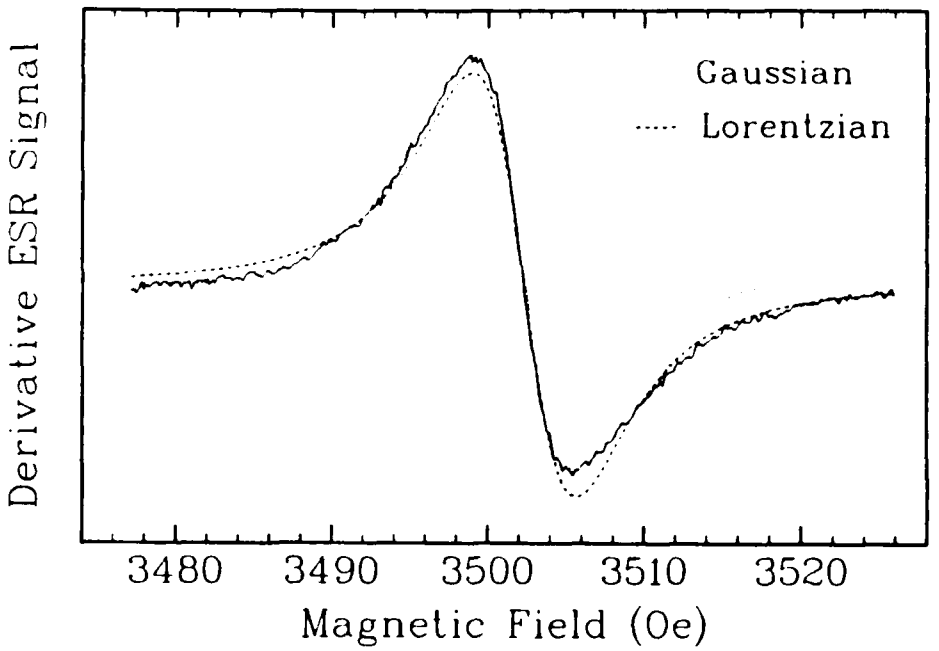

Figure 1. Comparison of Lorentzian and Gaussian lineshape fits to 5 K EPR spectrum for ^{11}B-implanted CdTe sample C3-B with magnetic field along <100>-direction.

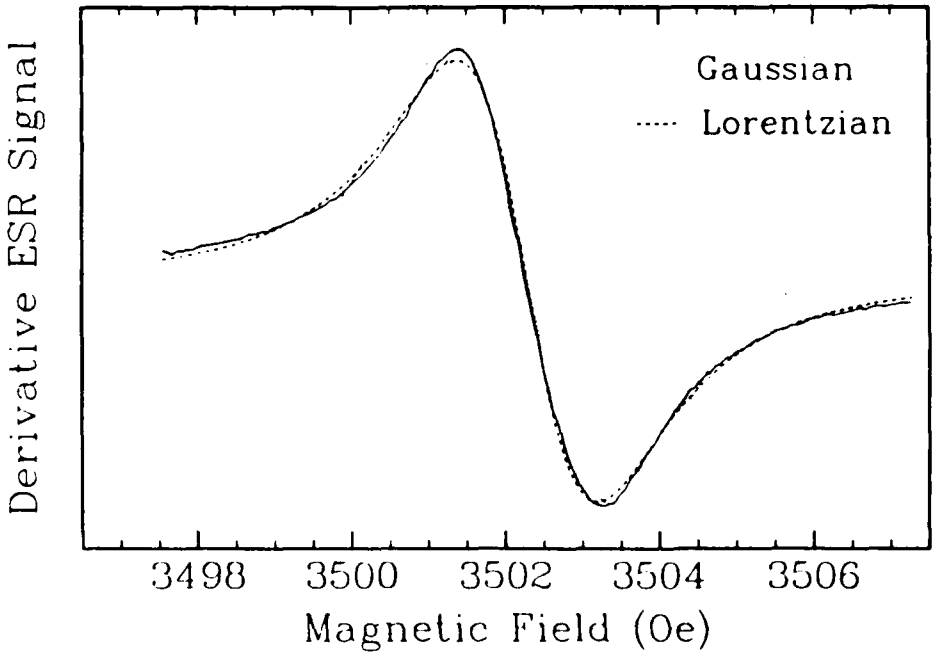

Figure 2. Comparison of Lorentzian and Gaussian lineshape fits to 4 K EPR spectrum for ^{11}B-implanted $Hg_{0.68}Cd_{0.32}Te$ sample H6 with magnetic field along <110>-direction.

TABLE IV. SUMMARY OF EPR PARAMETERS FOR BORON-IMPLANTED (1×10^{16} ions/cm^2) $Hg_{1-x}Cd_xTe$ CRYSTALS AND PARAMETERS FOR DANGLING-BOND DEFECTS IN ION-IMPLANTED Si AND GaP

SAMPLE	x	T (K)	ANNEALING TREATMENT	g-FACTOR	ΔH_{pp} (gauss)	FITTED LINESHAPE TYPE
C1	1.00	6	As Implanted	2.0008(20)	4.7	Lorentzian
C3-A	1.00	4.9	As Implanted	2.0005(20)	5.8	Lorentzian
C3-A	1.00	4.8	200°C, 1 hr	2.0009(20)	5.4	Lorentzian
C3-B	1.00	2	As Implanted	2.0026(1)	7.2	Lorentzian
H6	0.32	4	As Implanted	2.0028(1)	1.8	Lorentzian
H5	0.32	2	As Implanted	2.0028(1)	3.4	Dysonian
H5	0.32	2	200°C, 1 hr	2.0028(1)	2.4	Dysonian
Si[a]	--	77	None(280 keV P^+)	2.0059(5)	5.2(4)	Lorentzian
GaP[b]	--	77	None(200 keV N^+)	2.0032(4)	~6	Lorentzian

[a]Dangling-bond parameters from Ref. 10.
[b]Dangling-bond parameters from Ref. 11.

typically seen[8] in implanted $Hg_{1-x}Cd_xTe$. Furthermore, the g-factors in Table IV for the boron-implanted CdTe samples are distinctly different from the $g \approx 1.7$ values reported in Table II for the shallow donor states in chemically doped CdTe. The in situ illumination of the implanted crystals cooled to temperatures below ~ 10 K also did not generate any $g \approx 1.7$ signals that could be associated with shallow donors. The absence of hyperfine structure in the EPR spectra for the implanted $Hg_{1-x}Cd_xTe$ samples precludes a definitive determination of the defects. Table II does contain a defect with similar parameters--namely, vacancies on the tellurium sites. However, this postulated assignment has not been substantiated and may not be correct.

A more detailed examination of $Hg_{0.68}Cd_{0.32}Te$ sample H6 in which the boron ions were implanted into a polished <110>-face revealed some interesting orientation and temperature effects. When this sample was cooled to 2 K, the lineshape of the implantation defect became distinctly anisotropic as shown in Fig. 3. A partially resolved two-line spectrum was obtained when the crystal was rotated ~45° from the <110>-axis. Although this lineshape may reflect hyperfine interactions, it is not readily interpreted from the natural distribution of the Hg, Cd, or Te isotopes or the expected quadruplet for the implanted ^{11}B ions. Consequently, we currently believe that two (or more) independent defect centers with slightly different g-factors are responsible for the 2 K EPR spectrum in Fig. 3. The collapse of the two-component line into a single peak as the temperature increases is shown in Fig. 4. A symmetric and nearly Lorentzian lineshape is observed above 6 K, where the ΔH_{pp} values systematically decrease from 1.7 gauss to 1.2 gauss as the temperature is raised to 25 K. This behavior in ΔH_{pp} is consistent with a thermally activated process in which the paramagnetic spin can hop between two inequivalent locations. Although the identities of these defects are presently unknown, they are probably located on either individual complexes or in closely spaced independent centers. This general behavior has been reproduced with a second $Hg_{0.7}Cd_{0.3}Te$ sample (i.e., H5); however, the ΔH_{pp} values were too large for the implanted CdTe samples to detect two distinct components in the lineshapes. Further low-temperature EPR experiments are required to clarify the nature of the defects responsible for these signals.

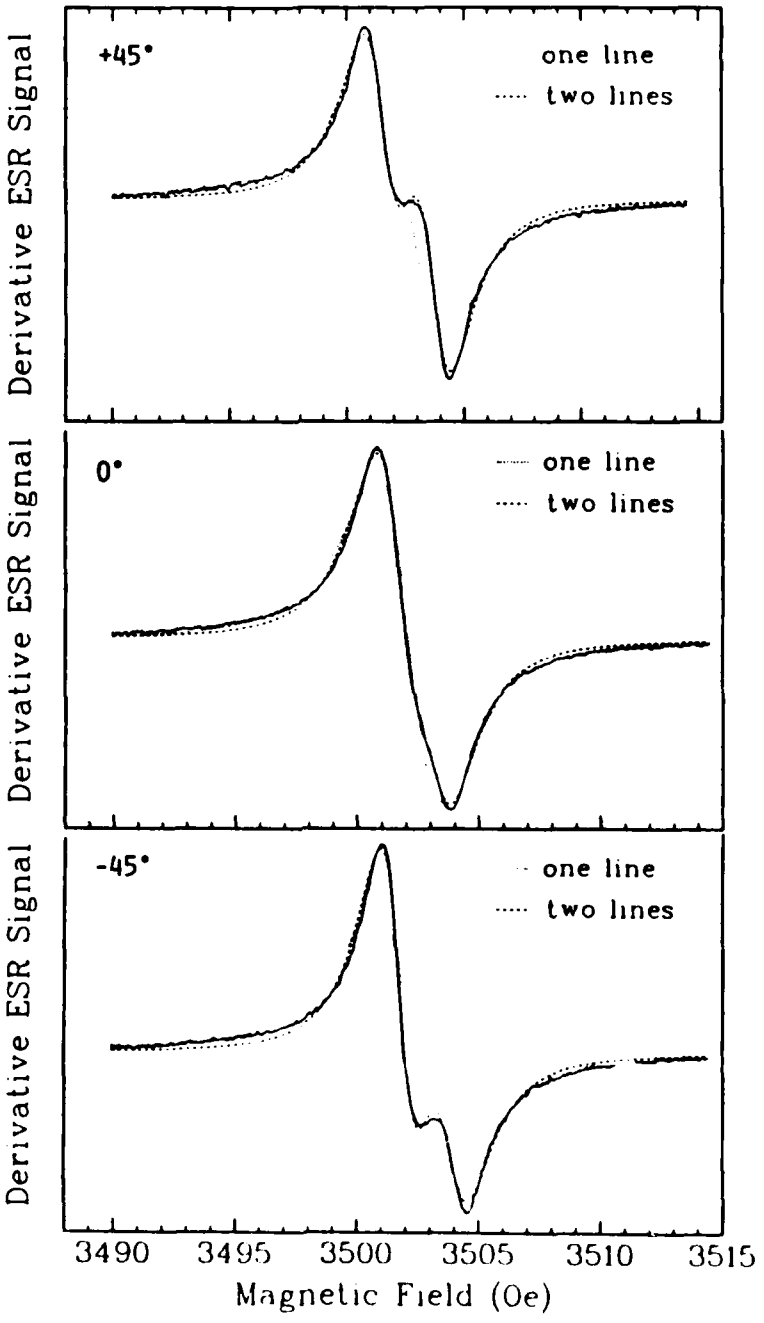

Figure 3. Orientation dependence of EPR lineshapes at 2 K for ^{11}B-implanted $Hg_{0.68}Cd_{0.32}Te$ sample H6 where 0° is parallel to <110>-direction.

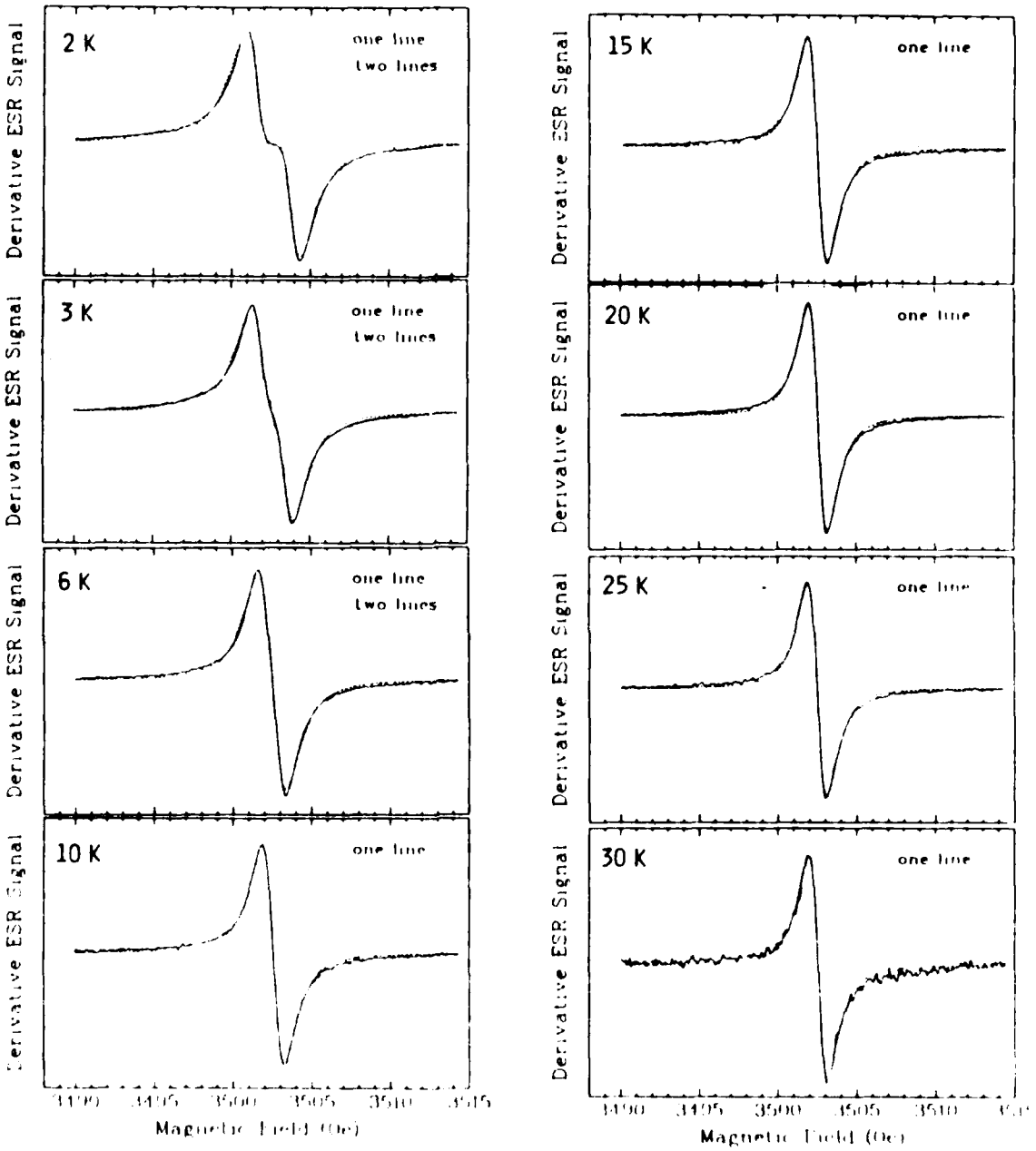

Figure 4. Temperature dependence of lineshapes for ^{11}B-implanted $Hg_{0.68}Cd_{0.32}Te$ sample where two-line and one-line analyses are compared.

Studies of the effects of thermal anneals on the EPR spectra generated by ion implantation have been initiated. The first results were obtained with 200°C anneals for one hour under flowing nitrogen gas. Although no significant changes in the g-factors or signal amplitude were apparent, changes in the lineshape and ΔH_{pp} were noted as shown in Table IV. The significance of these changes on the nature and distribution of the paramagnetic centers created by the boron implantation remains obscure.

In summary, the present initial studies have demonstrated that useful EPR measurements are possible in $Hg_{1-x}Cd_xTe$ crystals although tuning problems can occur because of the high electrical conductivities in the narrower gap materials that are n-type or have been implanted. Whereas paramagnetic transition metals were found in some undoped CdTe samples, no EPR signals were obtained from any p-type $Hg_{0.7}Cd_{0.3}Te$ in contrast to the unidentified paramagnetic species recently mentioned by Jones, et al.[7] Heavy dose (i.e., 10^{+16} ions/cm^2) boron ion implants generated "free-electron"-like EPR signals in both CdTe and $Hg_{0.7}Cd_{0.3}Te$. For identical implant conditions, a larger paramagnetic defect concentration is indicated from the $Hg_{0.7}Cd_{0.3}Te$ samples. Although the identities of these new defects have not been established, they do not appear to correspond to the shallow donor species previously studied in chemically doped CdTe. In fact, the characteristics of the EPR spectra for the boron-implanted $Hg_{1-x}Cd_xTe$ appear to be very similar to the dangling-bond centers found in other damaged or amorphous semiconductors.

REFERENCES

1. J. E. Wertz and J. R. Bolton, Electron Spin Resonance - Elementary Theory and Practical Applications (McGraw-Hill, New York, 1972).

2. C. P. Poole, Electron Spin Resonance - A Comprehensive Treatise on Experimental Techniques, 2nd Edition (John Wiley, New York, 1983).

3. R. S. Title, in Physics and Chemistry of II-VI Compounds, edited by M. Aven and J. S. Prener (American Elsevier, New York, 1967) p. 265.

4. J. Schneider, in II-VI Semiconducting Compounds, edited by D. G. Thomas (Benjamin, New York, 1967) p. 40.

5. J. W. Corbett, R. L. Kleinhenz, and N. D. Wilsey, in Defects in Semiconductors, edited by J. Narayan and T. Y. Tan (North-Holland, New York, 1981) p. 1.

6. A. K. Koh, D. J. Miller, and C. T. Grainger, Phys. Rev. B29, 4904 (1984).

7. C. E. Jones, et al., J. Vac. Sci. Technol. A3, 131 (1985).

8. G. L. Destefanis, Nucl. Instrum. Methods 209/210, 567 (1983).

9. T. W. Sigmon, Nucl. Instrum. Methods B 7/8, 402 (1985).

10. B. L. Crowder, R. S. Title, M. H. Brodsky, and G. D. Pettit, Appl. Phys. Lett. 16, 205 (1970).

11. T. Matsumori, K. Miyazaki, and S. Shigetomi, Appl. Phys. Lett. 42, 521 (1983).

12. H. Ryssel, et al., Phys. Status Solidi A 57, 619 (1980).

13. L. O. Bubulac, J. Cryst. Growth 72, 478 (1985).

LABORATORY OPERATIONS

The Aerospace Corporation functions as an "architect-engineer" for national security projects, specializing in advanced military space systems. Providing research support, the corporation's Laboratory Operations conducts experimental and theoretical investigations that focus on the application of scientific and technical advances to such systems. Vital to the success of these investigations is the technical staff's wide-ranging expertise and its ability to stay current with new developments. This expertise is enhanced by a research program aimed at dealing with the many problems associated with rapidly evolving space systems. Contributing their capabilities to the research effort are these individual laboratories:

Aerophysics Laboratory: Launch vehicle and reentry fluid mechanics, heat transfer and flight dynamics; chemical and electric propulsion, propellant chemistry, chemical dynamics, environmental chemistry, trace detection; spacecraft structural mechanics, contamination, thermal and structural control; high temperature thermomechanics, gas kinetics and radiation; cw and pulsed chemical and excimer laser development including chemical kinetics, spectroscopy, optical resonators, beam control, atmospheric propagation, laser effects and countermeasures.

Chemistry and Physics Laboratory: Atmospheric chemical reactions, atmospheric optics, light scattering, state-specific chemical reactions and radiative signatures of missile plumes, sensor out-of-field-of-view rejection, applied laser spectroscopy, laser chemistry, laser optoelectronics, solar cell physics, battery electrochemistry, space vacuum and radiation effects on materials, lubrication and surface phenomena, thermionic emission, photosensitive materials and detectors, atomic frequency standards, and environmental chemistry.

Computer Science Laboratory: Program verification, program translation, performance-sensitive system design, distributed architectures for spaceborne computers, fault-tolerant computer systems, artificial intelligence, microelectronics applications, communication protocols, and computer security.

Electronics Research Laboratory: Microelectronics, solid-state device physics, compound semiconductors, radiation hardening; electro-optics, quantum electronics, solid-state lasers, optical propagation and communications; microwave semiconductor devices, microwave/millimeter wave measurements, diagnostics and radiometry, microwave/millimeter wave thermionic devices; atomic time and frequency standards; antennas, rf systems, electromagnetic propagation phenomena, space communication systems.

Materials Sciences Laboratory: Development of new materials: metals, alloys, ceramics, polymers and their composites, and new forms of carbon; nondestructive evaluation, component failure analysis and reliability; fracture mechanics and stress corrosion; analysis and evaluation of materials at cryogenic and elevated temperatures as well as in space and enemy-induced environments.

Space Sciences Laboratory: Magnetospheric, auroral and cosmic ray physics, wave-particle interactions, magnetospheric plasma waves; atmospheric and ionospheric physics, density and composition of the upper atmosphere, remote sensing using atmospheric radiation; solar physics, infrared astronomy, infrared signature analysis; effects of solar activity, magnetic storms and nuclear explosions on the earth's atmosphere, ionosphere and magnetosphere; effects of electromagnetic and particulate radiations on space systems; space instrumentation.

END

8-87

DTIC